Are Global Renormalization Methods Capable of Locating Gas–Liquid Critical Points?[1]

J. A. White[2]

A global renormalization procedure used recently to calculate thermal volumetric properties near and to far from the critical point for two square-well fluids, widths 1.5 and 3.0, with accurately known critical points is here applied in an effort to determine where the critical point is located for three square-well fluids, widths 1.375, 1.75, and 2.0, for which accurate simulation data near the critical point are lacking. The present approach is suggested as an alternative to extrapolation methods that have been applied in the past and resulted in widely divergent predictions. A problem in the past has been knowing what to use as an effective critical point exponent, β_{eff}, for purpose of the extrapolation. The present renormalization calculations indicate that rather widely different behaviors of β_{eff} as a function of distance from the critical point can be expected for square wells of different width.

KEY WORDS: critical point; gas–liquid coexistence curve; global renormalization; square-well fluids.

1. INTRODUCTION

A global renormalization procedure has been applied recently to calculate thermal volumetric properties of a Lennard–Jones fluid [1] and of two square-well fluids [2], of width 1.5 and 3.0, for which the location of the gas–liquid critical point has been determined accurately by simulation methods. What if the location of the critical point is not yet known accurately? Can renormalization methods be used to find that location? This question is explored here for several square-well fluids, using the renormalization procedure together with recent accurate molecular dynamics (MD) results [3] for coexisting gas and liquid densities when

not close to the critical point. Because of the difficulty in performing simulations when close to the critical point, the data in the MD investigations were obtained at densities either less than 35% or more than 170% of the critical point density, and at temperatures all 5% or more below the critical point temperature. Then, based on the simulation data, estimates were made of the critical point temperature, density, and pressure for each square well. The values obtained for these critical point quantities differed substantially from estimates that had been made previously from Monte Carlo (MC) simulations [4] performed over similar ranges of density and temperature.

In the present investigation, new estimates are made for the critical point temperature, density, and pressure by assuming that thermal behavior is given by global renormalization theory once the square-well potential and three constant parameters internal to the (approximate) theory are specified. This provides an alternative to making—perhaps rather questionable—assumptions about effective critical point exponents to extrapolate from accurate simulation data to find the critical point.

In the work reported below, estimates have been made for the three numerical parameters internal to the theory to be used for each square well in order to make global renormalization calculations of contours of coexisting vapor and liquid densities. The calculated contours for each square well are then compared with the MD results [3] for that square well. The renormalization calculations provide also information about the temperature dependence of the effective critical point exponent, β_{eff}. Plots are presented to show how β_{eff} varies with temperature for each square well.

The renormalization procedure used in this investigation is indicated below in Section 2. Results are summarized in Section 3.

2. METHOD OF CALCULATION

The general renormalization procedure followed here was the same as that used in Ref. 2. For completeness and convenience of reference, the procedure is summarized here in Sections 2.1 and 2.2, with some details specific to the present investigation noted toward the end of Section 2.3.

2.1. RG Equations

In the global renormalization approach the free energy density, $f(T, \rho)$, of the fluid (Helmholtz free energy per unit volume) at temperature T and number density ρ is separated into repulsive and attractive parts. Beginning with $f_0(T, \rho) = f_{repul}(T, \rho)$, renormalization contributions are

computed for increasingly long fluctuation wavelengths, beginning with wavelength λ_1.

After n renormalizations ($n-1$ doublings of the initial fluctuation wavelength λ_1) the free energy density $f(T, \rho)$ is written as

$$f(T, \rho) \simeq f_n(T, \rho) - \rho^2 a(T, \rho) \tag{1}$$

where, for each n (>0),

$$f_n(T, \rho) = f_{n-1}(T, \rho) + \delta f_n(T, \rho) \tag{2}$$

The $-\rho^2 a(T, \rho)$ is the contribution of the attractive interactions to the free energy density in mean field approximation. The increment $\delta f_n(T, \rho)$ at each order n is

$$\delta f_n(T, \rho) = \frac{1}{\beta V_n} \ln \frac{I_{n,l}(T, \rho)}{I_{n,s}(T, \rho)} \tag{3}$$

Here $\beta = 1/(k_B T)$, where k_B is Boltzmann's constant, V_n is the averaging volume, $V_n = (z\lambda_n/2)^3$, and the $I_{n,s}(T, \rho)$ and $I_{n,l}(T, \rho)$ are integrals over the amplitudes of the wave packets of fluctuations of wavelengths $\lambda \simeq \lambda_n = 2^{n-1}\lambda_1$:

$$I_{n,i}(T, \rho) = \int_0^{\rho'} dx\, e^{-\beta V_n D_{n,i}(T, \rho, x)}, \qquad i = s, l \tag{4}$$

In Eq. (4) the upper density limit, ρ', is the smaller of ρ or $\rho_{\max} - \rho$, where $\rho_{\max}$ does not exceed the density of closest packing of the molecules. And each $D_{n,i}(T, \rho, x)$ is given by

$$2D_{n,i}(T, \rho, x) = \hat{f}_{n-1,i}(T, \rho + x) + \hat{f}_{n-1,i}(T, \rho - x) - 2\hat{f}_{n-1,i}(T, \rho) \tag{5}$$

where, for $i = l$,

$$\hat{f}_{n-1,l}(T, \rho) = f_{n-1}(T, \rho) \tag{6}$$

and for $i = s$,

$$\hat{f}_{n-1,s}(T, \rho) = f_{n-1}(T, \rho) - \rho^2 a_{\lambda_n}(T, \rho) \tag{7}$$

where

$$a_\lambda(T, \rho) = -\int d\mathbf{r}\, \cos(\mathbf{k} \cdot \mathbf{r})\, U_2(r)\, g_{\mathrm{repul}}(T, \rho, r) \tag{8}$$

In Eq. (8) $g_{\text{repul}}(T, \rho, r)$ is the radial distribution function for the repulsive interactions, $U_2(r)$ is one half the attractive portion of the two-body potential, and **k** is the wave vector of the fluctuation of wavelength $\lambda = 2\pi/k$. In the limit $n \to \infty$, for which $\lambda_n \to \infty$, the $a_\lambda(T, \rho)$ becomes simply the $a(T, \rho)$ in Eq. (1) above.

The procedure summarized above is capable of determining the free energy density completely, by taking fully into account details of the intermolecular potential and contributions made by fluctuations at all wavelengths, not limiting just to some aspects of contributions made by fluctuations of asymptotically long wavelengths.

2.2. Implementation for Square-Well Potential

The square-well potential is a spherically symmetric two-body potential which has the form

$$U(r) = U_{SW}(r) = \begin{cases} \infty, & r \leqslant \sigma \\ -\varepsilon, & \sigma < r < R\sigma \\ 0, & r \geqslant R\sigma \end{cases} \tag{9}$$

where r is the distance between the centers of the two molecules.

The free energy density $f_0(T, \rho) = f_{\text{repul}}(T, \rho)$ of the gas comprised of hard spheres of diameter σ is, apart from a contribution to $f_{\text{repul}}(T, \rho)/\rho$ dependent on temperature but independent of density, approximately

$$\frac{\beta f_{\text{repul}}}{\rho} = \frac{4y - 3y^2}{(1-y)^2} + \ln y \tag{10}$$

where $y = \frac{1}{6}\pi\rho\sigma^3$. The pressure $P = \rho\, \partial f/\partial \rho - f$ calculated using $f = f_{\text{repul}}$ given by Eq. (10) yields, when multiplied by β/ρ, the Carnahan–Starling [5] expression for $Z = \beta P/\rho = PV/(RT)$, namely

$$Z_{\text{repul}} = \rho\, \frac{\partial}{\partial \rho}\left(\frac{\beta f_{\text{repul}}}{\rho}\right) = \frac{1 + y + y^2 - y^3}{(1-y)^3} \tag{11}$$

In evaluating Eq. (8), the $g_{\text{repul}}(T, \rho, r)$ was approximated as that for a gas of hard spheres, of diameter σ, in Percus–Yevick approximation [6]. And the attractive part of the potential, $U_2(r)$, was taken to be $\frac{1}{2}U_{SW}$ of Eq. (9) for all $r > \sigma$ and zero for $r \leqslant \sigma$.

With the above substitutions for the repulsive and attractive portions of the intermolecular potential, once σ, ε, and R of the potential and the

parameters λ_1 and z internal to the RG theory are specified, the $f(T, \rho)$ given by Eq. (1) is completely determined—apart from a contribution [noted above Eq. (10)] that depends only on temperature and does not contribute to the pressure—upon completion of n renormalizations.

2.3. Some Calculational Details

In the numerical calculations, the integrations were performed by the trapezoid rule, using equal size steps. Typically, 1000 steps were used for the calculation of each $a_\lambda(T, \rho)$, in Eq. (8). For the $g_{\text{repul}}(T, \rho, r)$ appearing in Eq. (8), the table in Ref. 6 was used, with interpolation when required. Equation (8) was evaluated for the twelve (dimensionless) densities $\rho\sigma^3 =$ 0.0, 0.1, 0.2,..., 1.1 for which tabulated values of g_{repul} were available [6], and a polynomial of fifth order in $\rho\sigma^3$ was fitted to each $a_\lambda(T, \rho)$ for use in Eq. (7), which needs to be evaluated at many intermediate densities in the range $0 < \rho\sigma^3 < 1.1$.

For use in the present investigation, the free energy density f was evaluated, at (dimensionless, $\rho\sigma^3$) density intervals of 0.001, for $0 < \rho\sigma^3 \leqslant$ 1.1; for the lower limit, a small value, $\rho\sigma^3 = 10^{-12}$, was used in place of

Table I. Estimated Location of Critical Point for Square Wells of Width 1.375, 1.5, 1.75, and 2

R	λ_1	z	ε/k_B	T_c	ρ_c^*	P_c	Z_c	Ref.[a]
1.375	4.0	0.86	1.022	0.969	0.378	0.083	0.228	W
				1.01	0.344	0.10	0.29	EH99
				0.974	0.355	0.105	0.30	V92
1.5	4.5	0.94	1.027	1.215	0.319	0.097	0.250	W
				1.27	0.306	0.11	0.30	EH99
				1.219	0.299	0.108	0.30	V92
				1.218	0.310	0.095	0.252	OP99
1.75	6.0	0.98	1.023	1.797	0.262	0.130	0.275	W
				1.79	0.267	0.12	0.25	EH99
				1.811	0.284	0.179	0.35	V92
2.0	7.0	0.95	1.031	2.671	0.256	0.191	0.280	W
				2.61	0.267	0.17	0.24	EH99
				2.764	0.225	0.197	0.32	V92
				2.684	0.235			M97

[a] W, This work, for the indicated choice of parameters λ_1, z, and ε/k_B. EH99, MD estimates, from Table III of Ref. 3. The value listed there for η_c has been multiplied by $6/\pi$ to convert it to ρ_c^*. V92, MC estimates from Table VI in Ref. 4. OP99, MC results listed in Table I of Ref. 7. M97, MC values for $N = 1364$ particles, from Table II of Ref. 8.

$\rho\sigma^3 = 0$ to avoid the logarithmic singularity in Eq. (10). The integrand in Eq. (4) was evaluated, by trapezoid rule, at the same dimensionless density intervals, 0.001, using for the maximum integration limit $\rho'\sigma^3 = \rho_{max}\sigma^3/2 = 1.1/2$. Smaller choices for that limit, down to $\rho'\sigma^3 = 0.9/2$, had almost no noticeable effect on the results obtained here. Four point interpolation was used to estimate f when calculating thermal properties at densities intermediate between those at which f had been evaluated.

Calculations of $f_n(T, \rho)$ were carried through to order $n = 9$. After the first few iterations of the recursion relations for increasing n, contributions δf_n decreased rapidly in size, with negligible contributions except very close to the critical point for $n > 6$. (Although contours of coexisting liquid and vapor densities change very little for $n > 6$, values obtained for β_{eff} close to the critical point are somewhat more sensitive to renormalization corrections, so calculations were continued to larger n until changes in β_{eff} were negligible to within 0.05% of the critical point temperature.)
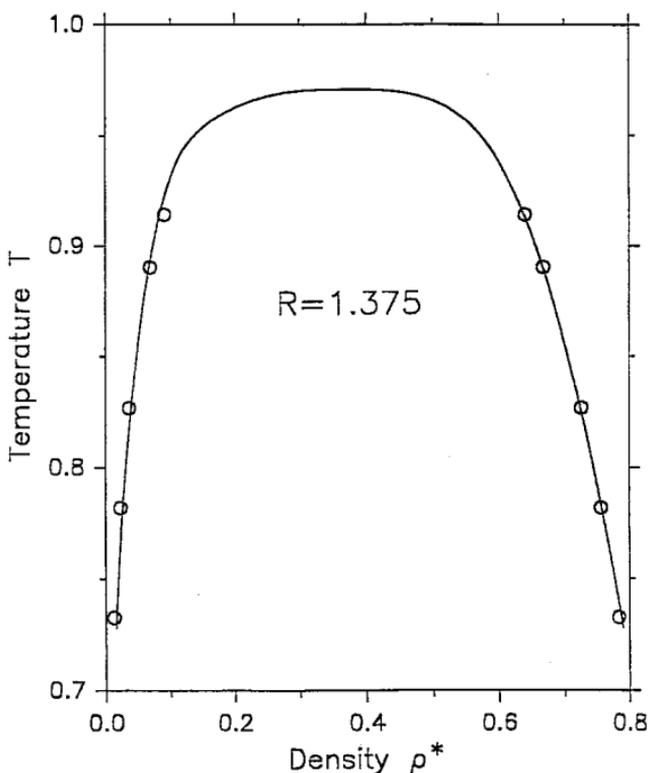
Fig. 1. Densities at the liquid–vapor coexistence curve for $R = 1.375$. Circles: MD simulations [3]. Solid line: RG calculations.

3. RESULTS

Renormalization calculations were performed as described above for square wells of width $R = 1.375$, 1.5, 1.75, and 2 to find P^* as a function of T^* and ρ^*, where $P^* = P\sigma^3/\epsilon$, $T^* = k_B T/\epsilon$, and $\rho^* = \rho\sigma^3 = N\sigma^3/V$ are the reduced (dimensionless) pressure, temperature, and density of the fluid. Results depended upon the choices made for the two internal parameters, λ_1 and z, required for the evaluation of Eq. (3). As in the earlier investigation [2] of square wells of width $R = 1.5$ and 3.0, the well depth, ε/k_B, used when carrying through the renormalization calculations, was subsequently assigned a value up to about 3% greater than the value $\varepsilon/k_B = 1$ used in the simulations. The choice for ε thus served as a third adjustable constant in the (approximate) renormalization calculations. (The R and $\sigma = 1$ used in the renormalization calculations were not changed from what had been used in the simulations.)

Critical points calculated for particular choices of the three adjustable constants are listed for each of the four square wells in Table I. The values
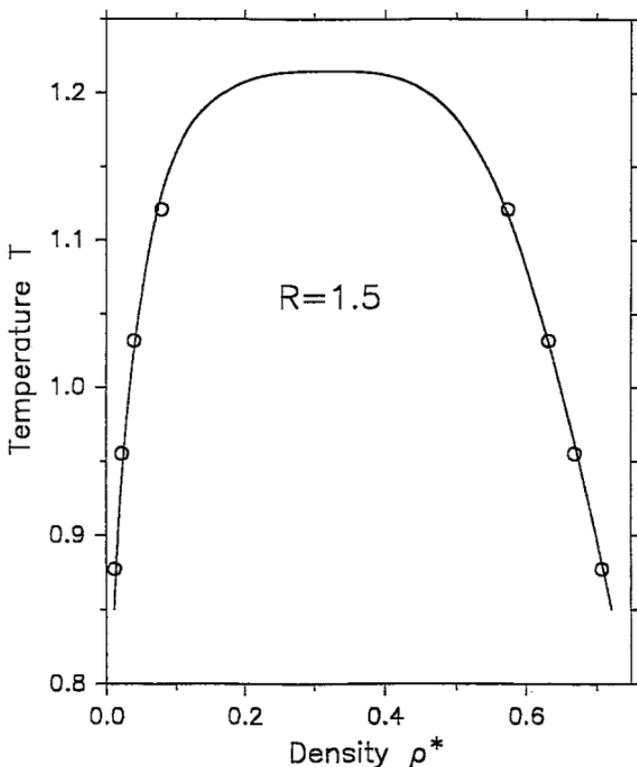
Fig. 2. Densities at the liquid–vapor coexistence curve for $R = 1.5$. Circles and solid line as in Fig. 1.

for λ_1 listed in the table range from 2.9 to 3.5 times the well width, $R\sigma$. The values listed in Table I for the other two renormalization constants, z and ε/k_B, were ones for which renormalization calculations gave reasonably good agreement with MD simulation results [3], as shown in Figs. 1 to 4. In those figures, as also in the table, the temperature "T" is $T = T^*$ for the simulation data, calculated for $\varepsilon/k_B = 1$, and is $T = \varepsilon T^*/k_B > T^*$ for the renormalization results, calculated using the values for ε/k_B listed, for each R, in the table.

Approximately equally good agreement with the MD results was obtained for choices of λ_1 that are 10 to 20% larger or smaller than those listed in Table I, provided the z and ε/k_B were suitably readjusted [9]. In particular, a 10% increase in λ_1 required, for the different width wells in the table, a 3 to 6% decrease in z and 0 to 0.3% increase in ε/k_B. Calculated values (for $\sigma = 1$, $\varepsilon/k_B \neq 1$) for T_c, ρ_c^*, and P_c then changed, for the different well widths, by $-(0.6 \pm 0.1)\%$, $+(0.2 \pm 0.7)\%$, and $-(3.5 \pm 1)\%$, respectively, and for $Z_c = P_c^*/(\rho_c^* T_c^*)$ by $-(3.3 \pm 1.3)\%$. These figures probably represent lower limits on uncertainties for the renormalization values for
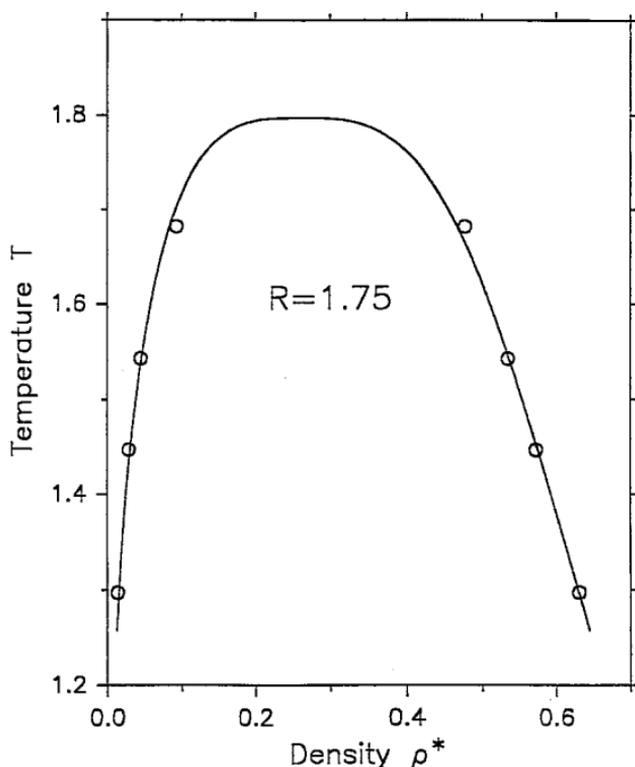
Fig. 3. Densities at the liquid–vapor coexistence curve for $R = 1.75$. Circles and solid line as in Fig. 1.
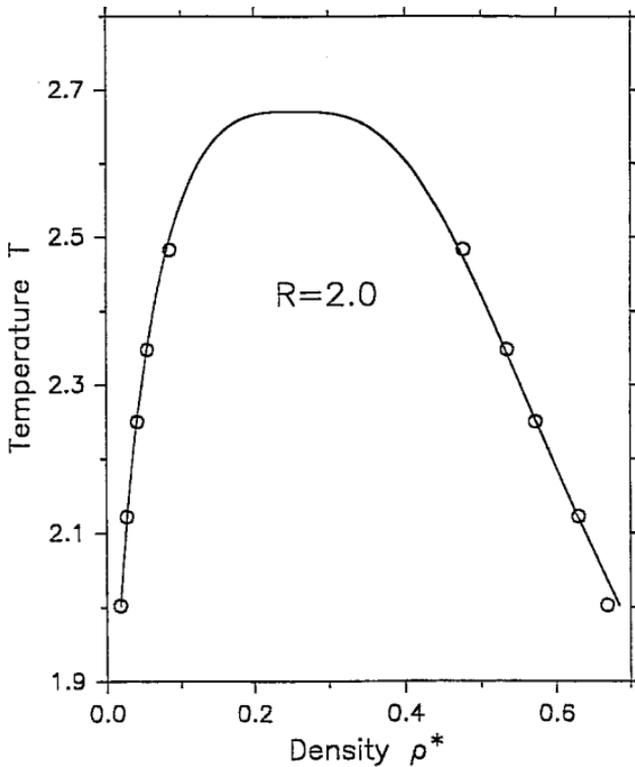
Fig. 4. Densities at the liquid–vapor coexistence curve for
$R = 2$. Circles and solid line as in Fig. 1.

the critical point constants listed in the table, which may be in error by somewhat more than $\pm 1\%$ for T_c, $\pm 1.5\%$ for ρ_c^*, and $\pm 5\%$ for P_c and Z_c.

In carrying through the renormalization calculations, it was found that the width, $\Delta\rho = \rho_{\text{liquid}} - \rho_{\text{vapor}}$, of the coexistence curve varied as a function of temperature distance, $\Delta T = T_c - T$, from the critical point for each square well with nearly the same critical point exponent $\beta \simeq 1/3$ for $\Delta T < 0.01 T_c$. But the local $\beta_{\text{eff}} = d\log|\Delta\rho/\rho_c|/d\log|\Delta T/T_c|$ for larger ΔT behaved quite differently for the different well widths. This is shown for the four square wells of widths $R = 1.375$ to $R = 2$ in Figs. 5a and 5b. The β_{eff} is seen there to have already quite different values for the different square wells when $\Delta T = 0.03 T_c$ (corresponding to $\log|\Delta T/T_c| \simeq -1.5$). Thus, it appears that the variation of β_{eff} with ΔT may need to be taken into account whenever extrapolating data obtained farther than about 1% below T_c in trying to estimate accurately the location of the critical point. And that variation of β_{eff} with ΔT is different for attractive wells of different width.
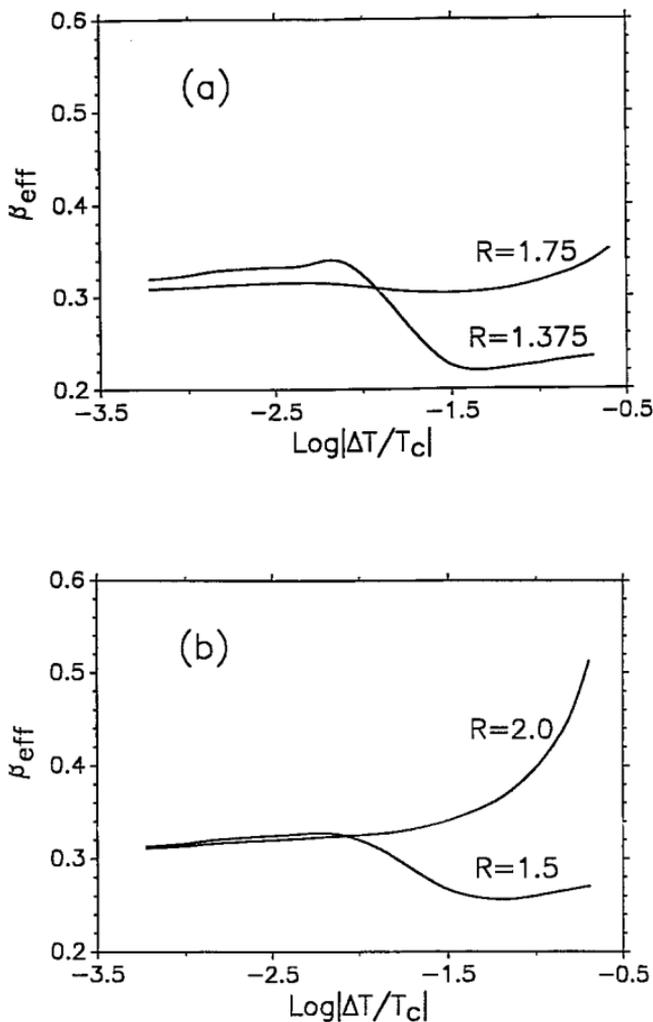
Fig. 5. Dependence of effective critical point constant $\beta_{\text{eff}} = d \log |\Delta\rho/\rho_c|/d \log |\Delta T/T_c|$, for width $\Delta\rho = \rho_{\text{liquid}} - \rho_{\text{vapor}}$ of coexistence curve, on temperature distance $\Delta T = T_c - T$ below the critical point for each of the four coexistence curves shown in Figs. 1–4.

REFERENCES

1. J. A. White, *J. Chem. Phys.* **112**:3236 (2000).
2. J. A. White, *J. Chem. Phys.* **113**:1580 (2000). Added in proof: Eq. 3, given incorrectly in that paper (with subscripts *s* and *l* interchanged), is corrected below.
3. J. R. Elliott and L. Hu, *J. Chem. Phys.* **110**:3043 (1999).
4. L. Vega, E. deMiguel, L. F. Rull, G. Jackson, and I. A. McLure, *J. Chem. Phys.* **96**:2296 (1992).
5. N. F. Carnahan and K. E. Starling, *J. Chem. Phys.* **51**:635 (1969).
6. G. J. Throop and R. J. Bearman, *J. Chem. Phys.* **42**:2408 (1965).

7. G. Orkoulas and Z. Panagiotopoulos, *J. Chem. Phys.* **110**:1581 (1999); see also G. Orkoulas, M. E. Fisher, and A. Z. Panagiotopoulos (in press).
8. E. de Miguel, *Phys. Rev. E* **55**:1347 (1997).
9. For a somewhat different choice of λ_1, z, and ε/k_B for width 1.5 square well, see Ref. 2. That reference also shows some calculations compared with accurate MC simulation data [7] for a square well of width $R = 3$. It may be of interest in the present context to note that for $R = 3$, a choice $\lambda_1 = 11 = 3.7R$, $z = 0.89$, $\varepsilon/k_B = 1.010$ gives $T_c = 9.975$, $\rho_c^* = 0.258$, $P_c = 0.845$, $Z_c = 0.332$, and coexistence and vapor pressure curves that differ only a little from those reported for $R = 3$ in Ref. 2, which were obtained using a quite different $\lambda_1 = 4.5 = 1.5R$, and $z = 0.95$, $\varepsilon/k_B = 1.014$.